A Novel Approach to Develop Grid Harmonic Model for Large-Scale Offshore WPP Integration to Turkey: A Before-Connection Analysis for Northwest Turkey

Sehri Nur Guler *‡, Kamil Cagatay Bayindir **, Adnan Tan ***

* Department of Electrical and Electronics Engineering, Ankara Yildirim Beyazit University, 06010, Ankara, Turkey

** Department of Electrical and Electronics Engineering, Ankara Yildirim Beyazit University, 06010, Ankara, Turkey

*** Department of Electrical and Electronics Engineering, Cukurova University, 01380,

Adana, Turkey

(195105108@ybu.edu.tr, kcbayindir@ybu.edu.tr, atan@cu.edu.tr)

‡ Sehri Nur Guler; Department of Electrical and Electronics Engineering, Ankara Yildirim Beyazit University, 06010, Ankara, Turkey, Tel: +90 312 906 2000,

Received: 07.11.2022 Accepted:27.03.2023

Abstract- Turkey has shown a lot of interest in renewable energy in recent decades. In Turkey today, there is a tremendous amount of power produced by wind power plants (WPPs). Large-scale offshore wind power plants (OWPPs) can be a solution to reduce the demand for electricity, keeping in mind that Turkey's installed wind power capacity is primarily from onshore stations. Due to its high wind speed capacity, the northwest of Turkey may be a suitable choice for a future OWPP installation. Large-scale OWPP connections in the area not only help to meet the region's energy needs, but they also provide advantages for the stability of the grid. However, the integration of such a large-scale power plant might cause serious harmonic stability issues. Although the system operator adopts and effectively utilizes a comprehensive model of the Turkish transmission grid, there is no harmonic equivalent model of the transmission network, which is essential for harmonic assessments. In this study, an equivalent harmonic model for harmonic impedance analysis of a proposed large-scale OWPP connection to Trakya, northwest Turkey, has been constructed. A thorough model of the Trakya region is first created in order to determine the grid's essential resonance locations, and the remaining grid (beyond the two straits) is then represented using harmonic equivalents. Following these arrangements, the driving point and transfer impedances at three Point of Connection (PoC) busbars are calculated to create a harmonic bus impedance matrix. Utilizing the software DigSilent Power Factory, whole modelling and analysis procedure was performed.

Keywords Harmonics, Offshore wind power plants, Harmonic impedance analysis, Harmonic propagation in networks

1. Introduction

Northwest Turkey is one of the locations that are available for potential large-scale offshore wind power plant (OWPP) connections with its high wind speed capacity. Integration of such a power plant may be beneficial given that the northwest of Turkey has a remarkable energy demand. Despite the fact that connecting large-scale OWPPs offers several advantages, a thorough pre-evaluation process is required. When the harmonic effects of OWPPs are taken into account, the level of complexity is much higher. Executing the required simulations is one strategy for overcoming challenges in estimating harmonic effects related to OWPPs. However, until some adjustments are made, no simulation model is completely accurate. These adjustments depend on the modelling basis and scope. For harmonic studies, for instance, it is recommended to use more detailed models. The ability to get a huge amount of private information from manufacturers is a key factor in determining the level of detail for harmonic models. As a result, building an accurate harmonic model is a challenging procedure that frequently necessitates extensive background research.

A grid's harmonic reaction can be implemented by creating corresponding harmonic models. A key property for an equivalent harmonic grid is it provides all harmonic resonance points of a grid in a realistic manner. These resonance points describe the level of penetration for harmonic currents and voltages. The frequency dependencies of system components, particularly cables and transformers, should be included in generated harmonic models in order to show these resonance locations as explicitly as possible.

When performing simple simulations, lumped models are typically preferred for transmission lines. Although lumped models are seen to be adequate for fundamental simulations carried out over the entire network, they are inapplicable for electro-magnetic transient (EMT) studies or harmonic load flows executed in particular zones that are affected. In terms of harmonic studies, a transmission line modelled as lumped cannot

exhibit real harmonic characteristics. As a result, it is impossible to reveal questioned resonance locations, which are essential for a harmonic response analysis.

The upper limit for detailed modelling is set in accordance with transmission line length. Resonances are most likely to happen at points where line capacitance is large enough because they happen when they interact with the system's overall inductance. Resonances are hence more important for longer line lengths. Capacitance for overhead lines is lower than for cables. When comparing lines of the same voltage and length, cables have a capacitance that is 20 to 40 times larger [1], [2]. Because of this, the maximum distance for detailed modelling of overhead lines is 250 km, compared to just 3–4 km for cables. Given that cables are frequently used by OWPPs, as suggested in [3], modelling cables is essential for a harmonic study. For the Turkish transmission network, existing overhead lines can be as long as 230 km, and cables can be as long as 17 km. All overhead lines and cables specified in the study region were remodelled during this study, despite the fact that detailed cable modelling is more important in the Turkey example.

Transformers affect grid impedance in a resistive rather than an inductive way up to higher order harmonics, in contrast to overhead lines and cables. Transformers with frequency dependencies introduce noticeable attenuations at parallel impedance magnitudes, which decreases filter investment costs [4].

In the literature, many works focus on harmonic effects of OWPP connections. Some harmonic studies are concentrated on OWPP connections made via direct current (DC) links [5], [6], [7], different from these works an high voltafe alternating current (HVAC) connected OWPP is focus of interest at this study. Turkey has a detailed representation of all transmission network up to 36kV busbars constructed in DigSilent Power Factory. For this study existing model of Turkish transmission grid is improved further to provide a harmonic representation of it. Once the model is renewed no equivalents are used as in [8], [9], [10] whole detailed model of Trakya region is employed for rest of the study. Development of harmonic model process focus on two main elements of the network: lines and transformers. For each of these elements some modifications like definition of frequency depended characteristics have been applied.

In this study, a harmonic equivalent of the existing grid model of Turkey is developed for harmonic resonance point analysis of a potential OWPP connection to the Kıyıköy stated in Trakya Region / Turkey. Through the development process study is concentrated on Trakya region since a particular distance of the analysis point is adequate for detailed modelling as also advised in [1] and [4]. To localize the simulations firstly the grid is reduced to only Trakya region by using Reduction tool of DigSilent power factory by splitting from İstanbul and Dardanelle Bosphouruses. To reflect harmonic characteristics of the grid beyond the straits resistance and inductance response deduced from frequency sweep analysis for up to 30^{th} harmonic is modelled to the strait connection points. Once the grid is reduced to Trakya region, for the selected three PoC busbars (for connection of Kıyıköy OWPP), a detailed harmonic impedance analysis is conducted to acquire a well-defined Z-busbar of the grid. At the process of developing harmonic bus impedance matrix, both direct and transfer impedances calculated at three point of connections (PoCs) as in [11]. For mesh grids like Turkey Transmission Grid, parallel resonances are critical. Therefore main focus was on locations and magnitudes of parallel resonance points at this study as in [12]. To provide a deeper look into the resonance points, both phase and sequence domains are evaluated and similar patterns are questioned as in [13]. Through the study Reduction and Power Quality tools of DigSilent Power Factory software is used. Main contribution of the conducted study is producing first harmonic equivalent grid model of Turkish transmission network. In addition to this first harmonic before connection analysis is conducted for a large scale OWPP connection to the north-western part of Turkey.

The rest of the paper is given as sections with titles of System Description, Harmonic Domain Modeling, Building Z-Busbar Matrix and Conclusion. At System Description section, general working condition considerations are summarized, at Building Z-Busbar Matrix section results of the analysis and some background settings are given and at Conclusions section results and main contributions of whole work is stated briefly.

2. System Description

2.1. Transmission Grid on Northwest Turkey

Northwest of Turkey is rich in terms of industrial facilities, penetration of renewable power plants (especially wind power) and residents. Increasing count of industrial facilities at the region results in introduction of distortive effects to the grid. When high population at the region is taken into account, limitation of harmonic current emission becomes even more important. In terms of energy demand, region has a great need for power which is mainly mitigated by importing power from eastern and western side of Turkey. Since these energy transfer is made via overhead lines crossing over the two straits; İstanbul and Dardanelle Bosphouruses quality of the electricity service is strongly bounded to health and resilience of these transmission lines. Therefore, a novel source of energy like an offshore wind power plant connection can be a remedy for energy demand of the area. In addition to effects to the locals, energy tranquility at the region is also desirable as two main interconnection lines of Turkey is stated at the region. Connecting Turkey to Bulgaria and Greece, two transmission lines enable energy import and export between Turkey and Europe.

In terms of equipment, transmission of power is mainly done via overhead lines as in whole Turkey transmission network. Longest overhead line and underground cable of Turkish network is stated at the region. Especially for cables widest cable network and most complex connections to overhead line grid is also stated at Trakya Region. Since construction of power transmission lines is difficult in overly populated cities like İstanbul increasing interest to underground cable employment is not surprising. At the region transformers are used mostly as two winding and accommodated to step up or step down the voltage while auto transformers are mainly used for high voltage level power conversions.

2.2. Kıyıköy Offshore Power Plant

In decision process of selecting optimal location for a large scale OWPP to Turkey in [14] many factors from bathymetry to

biological environment effects are investigated and Kıyıköy is selected from other four candidate zones. Kıyıköy also has an easier connection to the network and a wind speed of greater than 8.75 m/s which made the location superior to the other options [14]. Total power generation capacity at the region is decided according to available connection points and costs of building a new transformer station at the region. According to conducted study a total generation capacity of 1.8 GW is estimated and due to connection limitations this capacity is divided into two phases as 900MW for each. Phase I of Kıyıköy OWPP is connected to busbar of Substation A and phase II is connected to busbars of Substation B and C as shown in the Fig.1.

3. Harmonic Domain Modelling

3.1. Modelling Approach

In process of developing a harmonic equivalent grid proximity to the point that is assessed is the main deciding factor. Depending on closeness to the connection point, network elements are re-modelled with additional frequency depended characteristics. In [1] 3 busbar proximity to the main analysis point is considered as adequate for detailed modelling. For this study this limit of 3 busbars is extended to a region and rest of the grid is represented with equivalents.

In the process of reducing the grid into Trakya region, firstly the full model of Turkish transmission grid split from two straits. Corresponding resistance and inductances are defined to strait connection busbars shown at the Fig.1 for all harmonic spectrum to represent characteristics of the rest of the grid. For separation of grids DigSilent Power Factory Software's Network Reduction Tool is used. With this separation Trakya grid is totally isolated from the rest of the network. To represent the other part of the grid equivalents are defined at strait connection busbars. To produce a reliable representation of the grid, a frequency sweep analysis is executed at these busbars. With the resistance and inductance values deduced from this frequency sweep analysis a realistic equivalent of the network is produced. Short circuit power of the grid is decided by previous years' measured short circuit current data and again added to the grid equivalents connected to the strait connection points. When the grid is totally reduced to Trakya region, inside of the Trakya region is re-modelled.

Producing a detailed model suitable to be used in harmonic studies is strongly depended to modelling grid elements by taking into account their frequency dependencies. Since defining exact frequency dependent characteristics is generally tied to reliable data provided by manufacturers it not so easy to develop an accurate grid model version. Therefore this type of studies are generally constructed with assumptions.

At this phase of study all cables, transformers and overhead lines stated at Trakya region are re-modelled by using geometric information and calculated characteristics. In cable and overhead line re-modelling process geometric information of each element is added to the model. For transformers, a calculated frequency dependent resistance characteristic is defined. At the end of the process, a detailed model of Trakya region is produced.

Produced detailed model of Trakya grid is employed at before connection analysis of Kıyıköy OWPP. Further frequency sweep

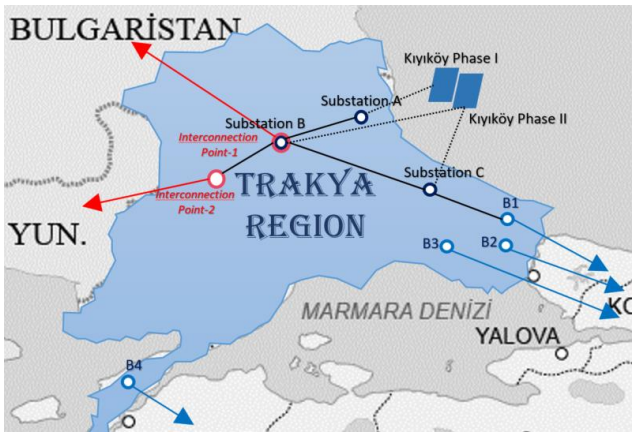

Fig. 1. Trakya Region and its connections with the rest of the grid. B1, B2, B3 and B4 are boundary busbars representing Trakya side ending points of the connection lines over the Bosphorus and Dardanelles. Substation A, B and C are denoting three connection busbars of OWPP (Strait connecting lines and grid interconnection lines are implemented with blue and red, respectively).

analysis is executed at three PoC busbars by taking into account both driving point and transfer impedances. A Z-busbar matrix is produced as an output of this frequency sweep analysis. General representation and equations of a Z-busbar model are given in (1) and (2).

At a Z-busbar matrix, impedances are calculated from dividing measured harmonic voltages to the flowed harmonic currents. For driving point impedances this ratio is constructed with harmonic voltages occurred by the flow of harmonic current at the same busbar to the flowed harmonic current at the same busbars while for transfer impedances this calculation is done by dividing measured harmonic voltage occurred because of a harmonic current flow at the neighboring busbar to the source harmonic current (i.e. ZAB is calculated as the harmonic voltage measured at Substation A divided by flowing harmonic current at Substation B).

$$Z_{BUS}(f) = \begin{bmatrix} Z_{AA}(f) & Z_{AB}(f) & Z_{AC}(f) \\ Z_{BA}(f) & Z_{BB}(f) & Z_{BC}(f) \\ Z_{CA}(f) & Z_{CB}(f) & Z_{CC}(f) \end{bmatrix}$$

$$Z_{AA}(f) = \left.\frac{V_A}{I_A}\right|_{I_B=I_C=0}$$

$$Z_{BB}(f) = \left.\frac{V_B}{I_B}\right|_{I_A=I_C=0} \quad (1)$$

$$Z_{CC}(f) = \left.\frac{V_C}{I_C}\right|_{I_A=I_C=0}$$

Where; $Z_{AA}(f)$, $Z_{BB}(f)$, $Z_{CC}(f)$ are implementing driving point impedance,

$$Z_{AB}(f) = Z_{BA}(f) = \left.\frac{V_A}{I_B}\right|_{I_A=I_C=0}$$

$$Z_{BC}(f) = Z_{CB}(f) = \left.\frac{V_B}{I_C}\right|_{I_A=I_B=0} \quad (2)$$

$$Z_{AC}(f) = Z_{CA}(f) = \left.\frac{V_C}{I_A}\right|_{I_B=I_C=0}$$

And, $Z_{AB}(f)$, $Z_{BC}(f)$, $Z_{AC}(f)$ are implementing transfer impedances between PoC busbars.

3.2 Harmonic Modelling of Overhead Lines and Cables

With the aim of producing a harmonic equivalent of Trakya grid all transmission lines are re-modelled. Instead of lumped π models, all overhead lines and cables are modelled by defining their geometric and phase-wise properties. In addition to the added properties, all lines are modelled with distributed parameters depending on lengths. General equations for distributed parameter-based line models are summarized in (3), (4) and (5).

At which;

$$\frac{Y'}{2} = \frac{Y}{2}\frac{tanh\frac{\gamma l}{2}}{\frac{\gamma l}{2}} \qquad (3)$$
$$Z' = Z\frac{sinh\gamma l}{\gamma l}$$

Where;

$$\gamma = \sqrt{zy} \qquad (4)$$
$$Z_c = \sqrt{z/y}$$

At which eventually results in the relations of;

$$Z' = Z_c sinh\gamma l \qquad (5)$$
$$Y' = \frac{1}{Z_c}tanh\frac{\gamma l}{2}$$

A comparison of lumped π models, distributed-geometric models and distributed-geometric and skin effect defined models are given in Fig.2. As seen from the figure only one resonance point is detected for the lumped π model, which is not so reliable for a line at this line length. When distributed model is used instead more than one resonance points are detected. To put the analysis to a closer to real scale skin effect is also defined and an understandable damp and shift is inspected for higher frequencies at this case.

Distributed models are used for both cables and overhead lines as given in above equations. Distributed parameter-based line models have the same properties with the equivalent π models since they are modelled as totally distributed, rather than π sections as used in [15].

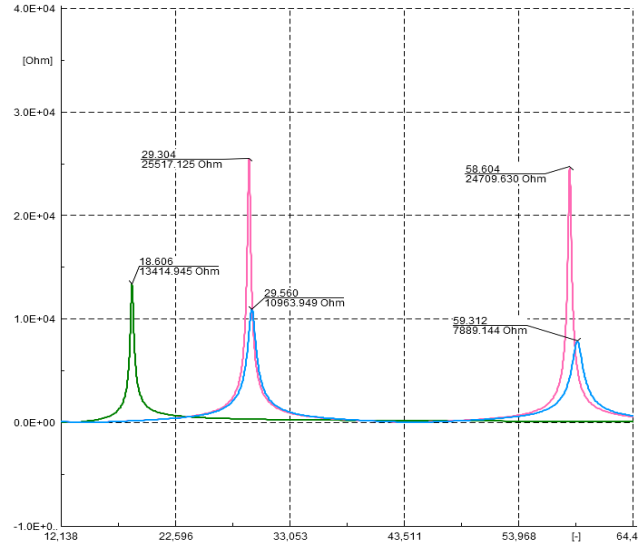

Fig. 2. Comparison of detailed and lumped line models (executed a line of 100km length) in terms of resonance points (results for lumped model shown as green, distributed model shown as pink and distrubuted and skin effect considered model is shown as blue)

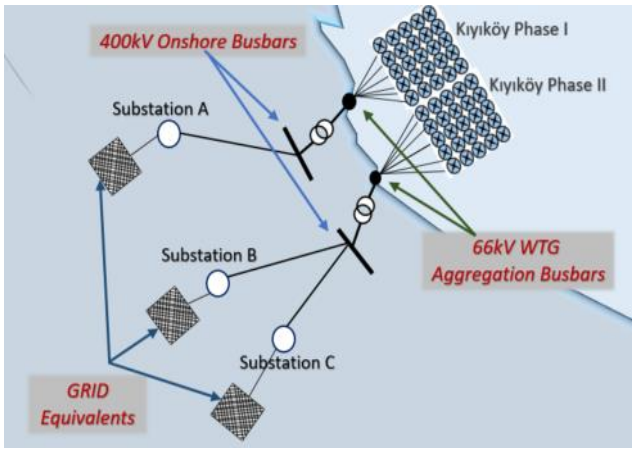

Fig. 3. Grid connections of the constructed system.

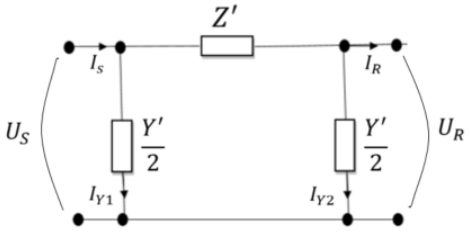

Fig. 4. Equivalent Pi model for transmission lines [1]

3.3 Harmonic Modelling of Transformers

Since inductance of transformers changes so slowly with frequency, it is appropriate to assume it as constant up to a certain level of frequency [4]. At a study which is focused on transformers it is verified with measurements that first resonances of a transformer occurs at approximately 10kHz [16]. Therefore for transformer harmonic domain modelling, introduction of frequency dependency of resistance is adequate.

In order to define frequency dependencies of resistances a frequency polynomial characteristic is defined to each high voltage level transformer by employing short circuit impedance (%Z) and X/R ratio data. At this study, different from the existing approach to transformer characteristic modelling [10], [16], [17] and [18]; a novel version of proposed model in [4] is produced and defined to each transformer with the help of Power Factory. Recalculation process of resistances are given below and a sample resistance characteristic taken from DigSilent Power Factory software is given in Fig.6 (with frequency in horizontal axis and resistance in vertical axis).

At first step %R(pu) values of transformers are calculated by the following equation;

$$R_{pu} = \frac{\%Z}{100}.\cos(\tan^{-1}[X/R]) \qquad (6)$$

And polynomial characteristic equation taken from Power Factory is defined;

$$y(f_h) = (1-a) + a(f_h/f_1)^b \qquad (7)$$

In above equation, coefficients of a=0,1 and b=1,99 taken from [19] is employed.

Fig. 5. Equivalent transformer model (Model 3, taken from [4])

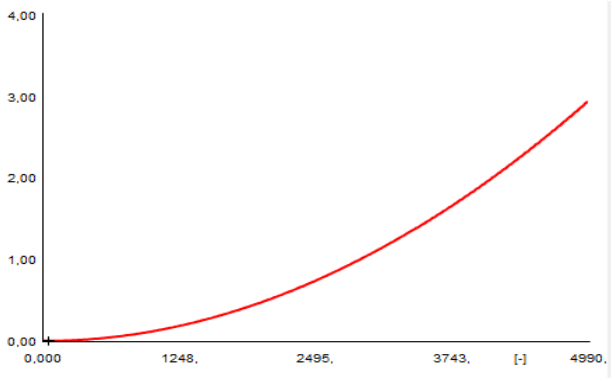

Fig. 6. A sample frequency dependent resistance characteristic for a transformer (taken from DigSilent related tool)

4. Building Z-Busbar Matrix

4.1 Detailed vs Lumped Model

After the remodeling process of transformers and transmission lines, there produced a detailed model version of Trakya grid. Comparisons of detailed and lumped models is made on Substation A busbar. Produced impedance graphs of this comparison analysis is given in Fig. 7 with phase domain approach. At the figure, change of location and magnitudes of resonance points is shown explicitly. As parallel resonances are critical for mesh grids like Turkish grid, outputs of analysis is evaluated with this approach. According to this, count of parallel resonance points was eight for lumped model and this is decreased to one for detailed model. In magnitudes there also inspected a change, as highest magnitude of resonances is decreased to 880,064 ohms (at 16th harmonic), from 2185,743 ohms (at 26th harmonic). First point of resonances is also changed from around 13th harmonic to the 16th harmonic, revealing that no critical harmonic exists in real state of the grid. Since first point of resonances is critical in terms of harmonic studies (because grid impedance is lower for lower order harmonics grid) this result of the study is remarkable.

4.2 Z- Busbar Matrix

Once the detailed model is prepared this model is used for process of developing Z-busbar matrix of the system and lumped model did not used from this point on. As stated above, for a sample Z-busbar production process, firstly all driving point and transfer impedances are calculated. Through this calculation the analysis is continued up to 1500Hz. Results of comparison of driving point and transfer impedances between Substation A and Substation B busbars is given in Fig.8. With this figure it can be concluded that a higher coherence is detected between Substation B driving point impedance and resulting transfer impedance.

Furthermore 27th harmonic is common for all busbars i.e. resonance at this harmonic in transfer impedance is supported by a harmonic current flowed in both of these two busbars. All driving point and transfer impedances between three PoC busbars with an addition of impedance angle graphs is given in Fig. 9. Vertical lines shown in angle diagrams of transmission impedance appear due to the change in angle from (-180) to (+180). Resulting parallel resonance points detected in Fig.9 is summarized in Table I and Table II as lower resolution version, at which red colored areas represents parallel resonance points (higher magnitudes). In Table I, positive and negative sequence parallel resonance points are given and in Table II zero sequence results are implemented.

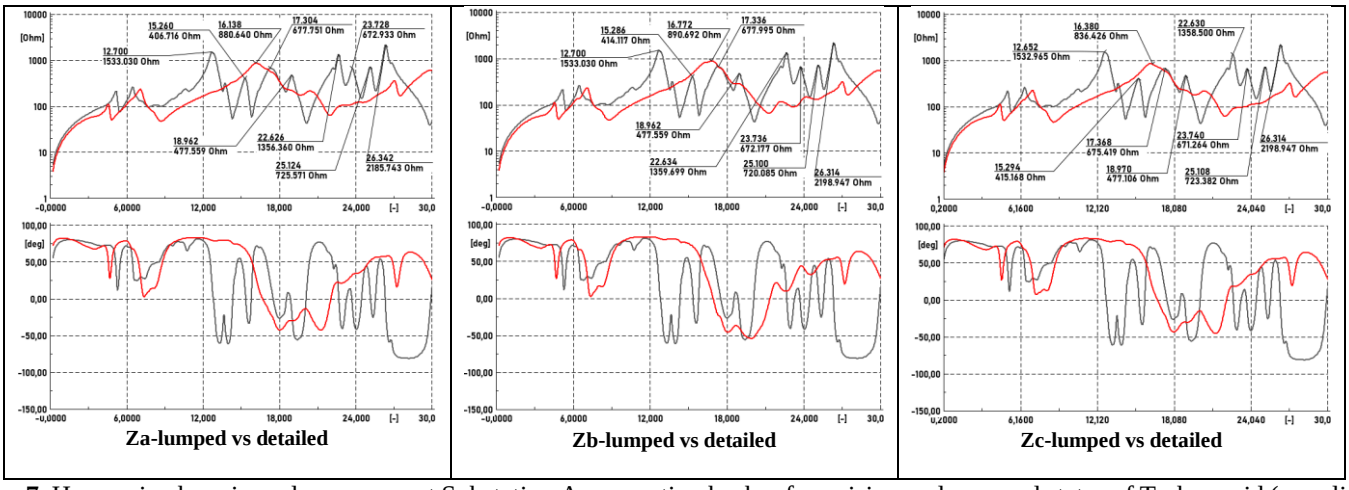

Fig. 7. Harmonic phase impedances seen at Substation A connection busbar for exising and renewed states of Trakya grid (grey line representing frequency sweep results for a all lumped grid scenario and red line representing results for when the Trakya grid is modelled in detail

According to Table I, the 8th, 14th and 27th harmonics are the most frequently observed resonance points. As a result of unbalanced network conditions resonance at the 27th could not be detected at phase domain although it is seen in sequence domain.

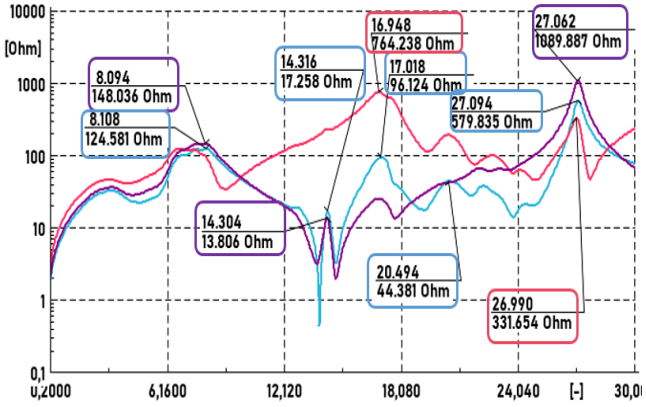

Fig. 8. Direct and transfer impedances for Substation A and Substation B busbars (direct impedance of Subs.A is implemented with red, direct impedance of Subs.B is implemented with purple and transfer impedance between these busbars is implemented with blue).

Table 1. Positive & Negative Sequence Harmonic Impedances Of All PoCs

Harmonic order	SubsA Driving Point Imp. (ohm)	SubsB Driving Point Imp. (ohm)	SubsC Driving Point Imp. (ohm)	Subs A<->B Trans. Imp. (ohm)	Subs A<->C Trans. Imp. (ohm)	Subs B<->C Trans. Imp. (ohm)
2	33,96	25,00	32,30	22,08	20,15	22,07
3	46,22	35,69	45,24	31,94	30,15	32,50
4	41,40	30,35	40,55	26,33	25,39	27,35
5	49,49	31,78	48,75	23,56	19,37	24,76
6	76,74	49,79	83,67	38,57	34,36	42,95
7	121,24	120,88	153,43	102,06	131,70	119,33
8	101,77	147,09	158,54	123,49	102,90	154,87
9	34,82	83,87	68,83	74,96	93,33	103,9
10	53,42	47,97	53,67	45,53	68,46	72,90
11	82,08	30,56	93,43	30,59	58,36	61,23
12	114,18	20,88	178,70	21,57	57,19	63,60
13	144,67	11,01	208,91	7,33	116,91	87,92
14	205,55	13,59	1669,6	17,26	177,93	111,19
15	276,17	4,17	418,12	7,51	63,63	19,98
16	462,48	15,67	187,08	37,45	121,57	40,08
17	759,47	25,36	175,90	95,86	220,57	45,13
18	396,86	15,48	154,36	35,92	86,64	13,05
19	140,47	27,35	116,44	18,45	41,61	20,39
20	159,41	39,66	95,28	39,34	22,36	25,61
21	151,11	46,72	80,51	33,44	17,41	29,70
22	80,56	66,86	68,76	34,56	13,72	36,30
23	94,58	65,97	63,84	28,30	6,74	34,83
24	62,13	72,32	59,05	17,18	5,02	33,93
25	46,64	108,67	48,76	21,26	12,22	47,46
26	108,76	215,18	32,47	74,06	32,04	84,33
27	333,58	1031,4	124,71	532,07	190,31	368,4
28	69,39	247,96	82,37	171,19	54,92	81,71
29	155,23	112,83	63,30	101,71	30,25	34,61
30	241,15	66,22	55,39	78,29	22,03	19,01

Table 2. Zero Sequence Harmonic Impedances Of All Pocs

Harmonic order	SubsA Driving Point Imp. (ohm)	SubsB Driving Point Imp. (ohm)	SubsC Driving Point Imp. (ohm)	Subs A<->B Trans. Imp. (ohm)	Subs A<->C Trans. Imp. (ohm)	Subs B<->C Trans. Imp. (ohm)
2	46,58	27,35	59,61	20,81	17,62	22,44
3	75,47	47,33	99,36	37,07	33,26	41,10
4	127,97	92,09	177,14	222,55	263,62	267,56
5	69,94	39,25	97,36	28,99	40,36	35,75
6	182,77	165,34	285,46	122,17	110,64	151,59
7	436,50	538,08	829,73	529,73	623,59	746,90
8	43,08	163,04	100,28	146,33	203,39	226,27
9	98,30	67,82	180,55	68,65	122,37	121,77
10	150,14	37,73	392,52	42,76	109,21	98,26
11	201,48	17,99	863,23	27,24	123,09	87,13
12	261,72	13,35	1475,4	8,72	70,67	136,47
13	344,53	13,15	984,20	8,97	62,98	53,74
14	452,98	28,40	537,97	35,25	81,66	64,78
15	736,55	51,24	363,25	81,28	128,96	77,44
16	1556,64	67,60	312,37	238,68	252,17	76,28
17	888,85	40,54	285,51	153,46	143,51	33,59
18	340,37	64,33	232,66	72,02	56,39	44,18
19	446,99	83,68	204,39	115,69	77,77	48,32
20	243,44	115,72	178,02	77,15	47,85	57,15
21	96,66	173,35	159,13	39,24	24,24	76,17
22	85,98	142,33	154,73	21,90	10,33	56,15
23	171,30	208,74	137,55	69,41	21,19	73,98
24	272,79	348,13	138,52	203,23	63,77	112,21
25	294,95	260,47	147,22	183,91	53,84	77,00
26	370,49	163,15	135,76	153,97	44,47	44,86
27	358,05	103,43	126,57	96,79	20,94	28,01
28	572,95	66,29	117,53	77,38	16,90	17,00
29	998,23	50,38	109,58	93,52	21,21	11,98
30	1531,44	69,14	103,16	195,19	44,17	15,62

5. Conclusion

With this study a detailed before connection analysis is executed for a large scale OWPP connection to the North western part of the Turkish grid. In order to do the analysis with a closer to real approach, existing model of Trakya grid is changed with a detailed harmonic equivalent model. In process of producing harmonic grid, all transmission lines and transformers are re-modelled by defining frequency dependent characteristics and by adding geometric information of elements. Once the detailed model is developed, lumped and detailed versions of the network is compared by assessing distribution of harmonic impedance points. As a result of this comparison it is concluded that locations and magnitudes of resonances are strongly dependent to network design level of detail. As a further step a Z-busbar matrix is produced by employing detailed model. With the help of produced Z-busbar matrix all critical resonance points are revealed both for individual busbars and also for transfer impedances between busbars.

Acknowledgements

This study is part of the "Offshore Wind Farms Large-Scale Integration in Turkey – WindFlag" project (www.windflag.et.aau.dk) funded by DANIDA Fellowship Centre and the Ministry of Foreign Affairs of Denmark to conduct research in growth and transition countries under the grant no. 19-M03-AAU.

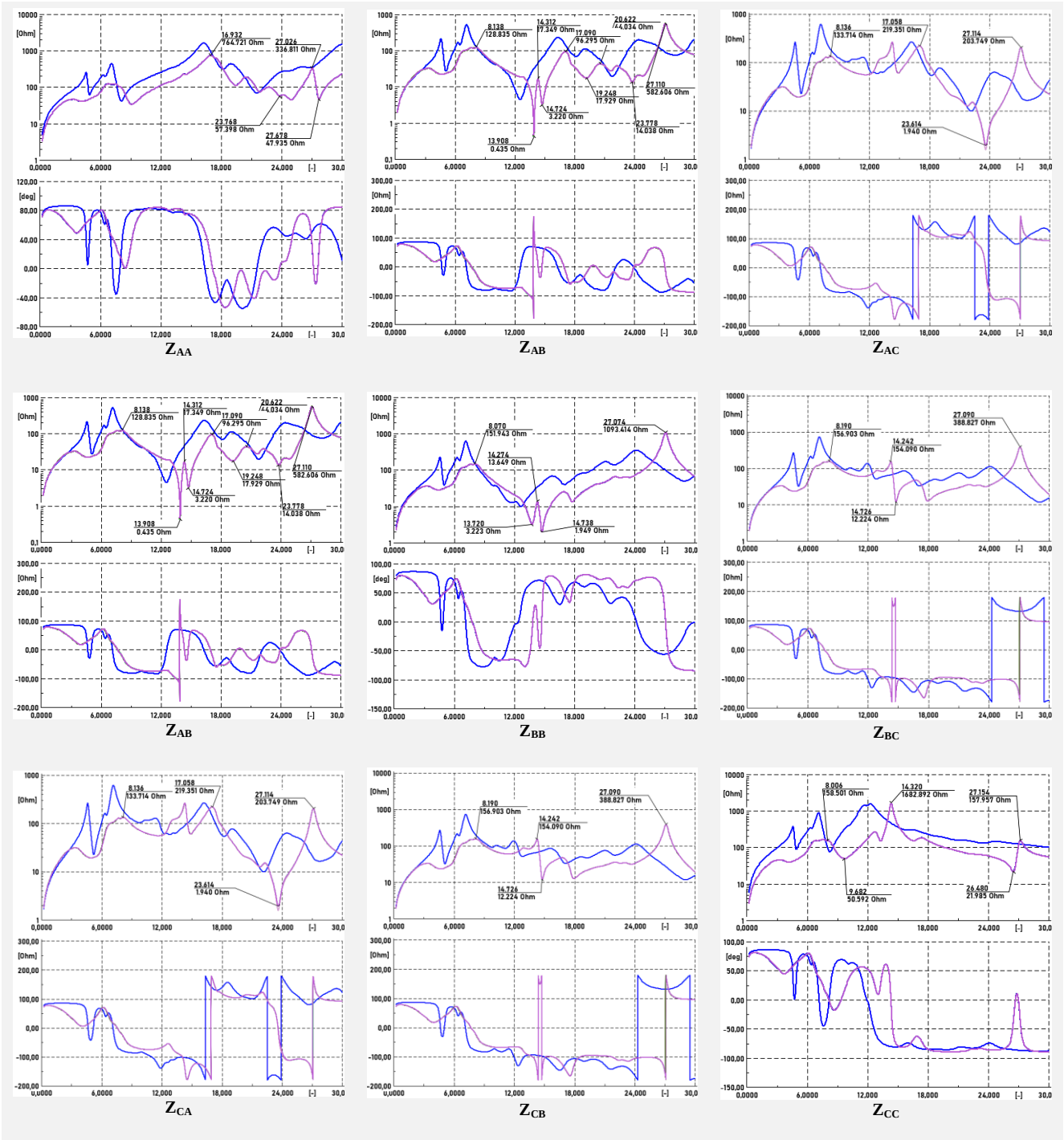

Fig. 9. Direct and transfer impedances for three PoC i.e. Z_{AA} is direct impedance for Substation A and Z_{AB} and Z_{AC} are transfer impedances between Substation A - Substation B and Substation A - Substation C respectively. Each graph is given with an additional impedance angle graph at the bottom and purple line represents positive and negative sequences and blue line is denoted for zero sequence.

References

[1] J. J. Grainger and W. D. Stevenson JR, Power System Analysis. McGraw-Hill.

[2] H. A. Brantsæter, 'Harmonic Resonance Mode Analysis and Application for Offshore Wind Power Plants', p. 112.

[3] C. Medina, C. R. M. Ana, and G. González, 'Transmission Grids to Foster High Penetration of Large-Scale Variable Renewable Energy Sources – A Review of Challenges, Problems, and Solutions', IJRER, no. Vol12No1, 2022, doi: 10.20508/ijrer.v12i1.12738.g8400.

[4] 'Network modelling for harmonic studies', p. 241.

[5] L. Yang, Z. Xu, L. Feng, Z. Zhang, Z. Xu, and F. Xing, 'Analysis on Harmonic Resonance of Offshore Wind Farm Transmitted by MMC-HVDC System', in 2019 IEEE Innovative Smart Grid Technologies - Asia (ISGT Asia), Chengdu, China, May 2019, pp. 2296–2301. doi: 10.1109/ISGT-Asia.2019.8881373.

[6] Y. Zhang, C. Klabunde, and M. Wolter, 'Harmonic Resonance Analysis for DFIG-based Offshore Wind Farm with VSC-HVDC Connection', in 2019 IEEE Milan PowerTech, Milan, Italy, Jun. 2019, pp. 1–6. doi: 10.1109/PTC.2019.8810495.

[7] M. Cheah-Mane, L. Sainz, E. Prieto-Araujo, and O. Gomis-Bellmunt, 'Impedance-based analysis of harmonic instabilities in HVDC-connected Offshore Wind Power Plants', International Journal of Electrical Power & Energy Systems, vol. 106, pp. 420–431, Mar. 2019, doi: 10.1016/j.ijepes.2018.10.031.

[8] M. Quester, V. Yellisetti, F. Loku, and R. Puffer, 'Assessing the Impact of Offshore Wind Farm Grid Configuration on Harmonic Stability', in 2019 IEEE Milan PowerTech, Milan, Italy, Jun. 2019, pp. 1–6. doi: 10.1109/PTC.2019.8810843.

[9] P. Eguía, G. Gil, R. RodrÍguez-Sanchez, M. Haro-Larrode, and A. Gil de Muro, 'Characterization of network harmonic impedance for grid connection studies of renewable plants', REPQJ, vol. 1, pp. 686–691, Apr. 2018, doi: 10.24084/repqj16.434.

[10] L. Depla, 'Harmonic Interactions in HVAC-Connected Offshore Windfarms', Master in Engineering, Universitat Polit`ecnica de Catalunya, 2019.

[11] S. K. Chaudhary et al., 'Harmonic Analysis and Active Filtering in Offshore Wind Power Plants', p. 6.

[12] K. N. B. Md. Hasan, K. Rauma, A. Luna, J. I. Candela, and P. Rodriguez, 'Harmonic Compensation Analysis in Offshore Wind Power Plants Using Hybrid Filters', IEEE Trans. on Ind. Applicat., vol. 50, no. 3, pp. 2050–2060, May 2014, doi: 10.1109/TIA.2013.2286216.

[13] C. F. Jensen, 'Harmonic background amplification in long asymmetrical high voltage cable systems', Electric Power Systems Research, vol. 160, pp. 292–299, Jul. 2018, doi: 10.1016/j.epsr.2018.03.009.

[14] E. Caceoğlu, H. K. Yildiz, E. Oğuz, N. Huvaj, and J. M. Guerrero, 'Offshore wind power plant site selection using Analytical Hierarchy Process for Northwest Turkey', Ocean Engineering, vol. 252, p. 111178, May 2022, doi: 10.1016/j.oceaneng.2022.111178.

[15] S. A. Papathanassiou and M. P. Papadopoulos, 'Harmonic Analysis in a Power System with Wind Generation', IEEE Trans. Power Delivery, vol. 21, no. 4, pp. 2006–2016, Oct. 2006, doi: 10.1109/TPWRD.2005.864063.

[16] I. A. Aristi, 'Switching overvoltages in off- shore wind power grids.', p. 451, 2011.

[17] A. M. Meinich, 'Harmonic Propagation and Production in Offshore Wind Farms', p. 104.

[18] Ł. H. Kocewiak, I. A. Aristi, B. Gustavsen, and A. Hołdyk, 'Modelling of wind power plant transmission system for harmonic propagation and small-signal stability studies', IET Renewable Power Generation, vol. 13, no. 5, pp. 717–724, Apr. 2019, doi: 10.1049/iet-rpg.2018.5077.

[19] C. F. Flytkær, 'Power System Component Harmonic Modelling'. Harmonics in Power Electronics and Power Systems, 29-31 October.